Experimental Neurology 314 (2019) 1–8

Contents lists available at ScienceDirect

Experimental Neurology

journal homepage: www.elsevier.com/locate/yexnr

Research paper

Activation of the hypothalamic paraventricular nucleus by acute intermittent hypoxia: Implications for sympathetic long-term facilitation neuroplasticity

Nadia Oliveira Maruyama[a], Nathan C. Mitchell[a], Tamara T. Truong[a], Glenn M. Toney[a,b,*]

[a] Department of Cellular and Integrative Physiology, University of Texas Health Science Center at San Antonio, San Antonio, TX 78229, USA
[b] Center for Biomedical Neuroscience, University of Texas Health Science Center at San Antonio, San Antonio, TX 78229, USA

ARTICLE INFO

Keywords:
Sympathetic nerve activity
Neural plasticity
Anxiety
Depression
Hypertension

ABSTRACT

Exposure to acute intermittent hypoxia (AIH) induces a progressive increase of sympathetic nerve activity (SNA) that reflects a form of neuroplasticity known as sympathetic long-term facilitation (sLTF). Our recent findings indicate that activity of neurons in the hypothalamic paraventricular nucleus (PVN) contributes to AIH-induced sLTF, but neither the intra-PVN distribution nor the neurochemical identity of AIH responsive neurons has been determined. Here, awake rats were exposed to 10 cycles of AIH and c-Fos immunohistochemistry was performed to identify transcriptionally activated neurons in rostral, middle and caudal planes of the PVN. Effects of graded intensities of AIH were investigated in separate groups of rats ($n = 6$/group) in which inspired oxygen (O_2) was reduced every 6 min from 21% to nadirs of 10%, 8% or 6%. All intensities of AIH failed to increase c-Fos counts in the caudally located lateral parvocellular region of the PVN. c-Fos counts increased in the dorsal parvocellular and central magnocellular regions, but significance was achieved only with AIH to 6% O_2 ($P < 0.002$). By contrast, graded intensities of AIH induced graded c-Fos activation in the stress-related medial parvocellular (MP) region. Focusing on AIH exposure to 8% O_2, experiments next investigated the stress-regulatory neuropeptide content of AIH-activated MP neurons. Tissue sections immunostained for corticotropin-releasing hormone (CRH) or arginine vasopressin (AVP) revealed a significantly greater number of neurons stained for CRH than AVP ($P < 0.0001$), though AIH induced expression of c-Fos in a similar fraction (~14%) of each neurochemical class. Amongst AIH-activated MP neurons, ~30% stained for CRH while only ~2% stained for AVP. Most AIH-activated CRH neurons (~82%) were distributed in the rostral one-half of the PVN. Results indicate that AIH recruits CRH, but not AVP, neurons in rostral to middle levels of the MP region of PVN, and raise the possibility that these CRH neurons may be a substrate for AIH-induced sLTF neuroplasticity.

1. Introduction

Exposure to acute intermittent hypoxia (AIH) induces plasticity in neural circuits that govern sympathetic nerve activity (SNA). This plasticity, referred to as sympathetic long-term facilitation (sLTF), develops upon returning to continuous normoxia following AIH exposure and manifests as a progressive increase of SNA lasting for at least several hours (Dick et al., 2007; Kim et al., 2018; Xing and Pilowsky, 2010). AIH-induced sLTF is understood only on a rudimentary level, but has recently been linked to actions of the hormone angiotensin II (AngII) at the blood-brain-barrier deficient subfornical organ (SFO) of the forebrain and at arterial chemoreceptors of the carotid bodies (Kim et al., 2018). Consistent with this mechanism, our recent study revealed that AIH-induced sLTF is nearly prevented by prior chemical inhibition of the hypothalamic paraventricular nucleus (PVN) (Kim et al., 2018), which lies synaptically downstream of the SFO (Ferguson, 2009; Miselis, 1981) and carotid body chemoreceptor inputs (Coldren et al., 2017; Kim et al., 2018; King et al., 2012; King et al., 2015; Reddy et al., 2005; Reddy et al., 2007). Whether dependence of sLTF on PVN neuronal activity reflects an active role for PVN neurons in responding to AIH or a permissive role in which ongoing PVN neuronal discharge supplies a required 'background' level of synaptic excitation within sLTF circuitry is presently unknown.

Here, we quantified AIH-induced recruitment of PVN neurons by exposing awake rats to graded intensities of AIH and used immunostaining for the immediate early gene product c-Fos to map the

* Corresponding author at: Department of Cellular and Integrative Physiology, University of Texas Health Science Center at San Antonio, San Antonio, TX 78229, USA.
E-mail address: toney@uthscsa.edu (G.M. Toney).

https://doi.org/10.1016/j.expneurol.2018.12.011
Received 15 September 2018; Received in revised form 3 December 2018; Accepted 30 December 2018
Available online 31 December 2018

regional and rostro-caudal distribution of transcriptionally activated PVN neurons. Intermittent hypoxia has been linked to activation of endocrine and autonomic components of the stress axis (Hwang et al., 2017; Ma et al., 2008; Przygodda et al., 2017; Wang et al., 2004; Zoccal et al., 2007), and because stress axis activation can enhance specific forms of synaptic plasticity that may contribute to sLTF (Arango-Lievano et al., 2015; Peters et al., 2018; Schierloh et al., 2007), we used dual immunostaining to determine the extent to which individual AIH-activated (c-Fos positive) PVN neurons contained the stress-regulatory neuropeptides corticotropin releasing hormone (CRH) and arginine vasopressin (AVP). We found that AIH robustly induced c-Fos amongst CRH containing, but not AVP containing, neurons located in the rostral half of the PVN's medial parvocellular subdivision, suggesting this population of CRH neurons could contribute to AIH-induced sLTF neuroplasticity.

2. Methods

2.1. Animals and ethical approval

Studies used male Sprague-Dawley rats (250–380 g; Charles River Laboratories, Wilmington, DE) that were housed in a temperature-controlled room (22–23 °C) with a 14:10-h light-dark cycle. Rats consumed standard chow with *ad libitum* access to tap water. All experimental procedures conformed to National Institutes of Health Guidelines and were approved by Institutional Animal Care and Use Committee of the University of Texas Health Science Center at San Antonio.

2.2. Telemetric recording of arterial pressure and heart rate

Mean arterial pressure (MAP) and heart rate (HR) changes during exposure to sham or graded intensities of AIH were recorded by radio telemetry (Data Sciences International, Inc., Minneapolis, MN, USA) in unanesthetized and unrestrained rats. Telemetry transmitters (model HD-S10) were implanted using aseptic surgical technique as previously described (Bardgett et al., 2014a; Sharpe et al., 2013a; Sharpe et al., 2013b). Briefly, each rat was anesthetized with isoflurane (~3% in O_2), a laparotomy was performed and the gel-filled catheter of pre-sterilized transmitter was inserted into the abdominal aorta and affixed with tissue adhesive. The transmitter housing was sutured to the posterior abdominal wall and the laparotomy sutured closed. Upon regaining consciousness, each rat received injections of the antibiotic penicillin G (30,000 units) and the analgesic buprenorphine (50 μg/kg) before being returned to a clean home cage. Rats were allowed to recover from surgery for 7 days prior to experiments. Arterial pressure was sampled at 500 Hz during 10 s sampling period each minute while rats experienced sham AIH or AIH to 10%, 8% or 6% O_2.

2.3. Exposure to acute intermittent hypoxia

Each rat individually housed in its home cage was relocated to a custom-built Plexiglas chamber and allowed to acclimate at normoxia (21% O_2) for 5 days. Thereafter, rats were exposed to our previously described (Kim et al., 2018) AIH protocol (see Fig. 1A). Briefly, chamber O_2 was reduced by perfusion with N_2 from 21% to nadirs of 10%, 8% or 6% over a period of ~145 s. Chamber O_2 was then held near its nadir for ~35 s before being returned to ~21% by perfusion with room air over the next ~105 s. Episodes of hypoxia were separated by a period of normoxia lasting ~75 s such that the duration of each normoxia-hypoxia cycle averaged ~6 min, allowing for 10 cycles/h. For exposure to sham AIH, chamber O_2 was held continuously at 21% by alternately switching chamber perfusion between two sources of compressed room air. Fluctuations of O_2 during AIH were separately recorded from each chamber using an analog sensor (KE-25, Figaro GS YUASA, Japan). Signals were amplified (Kent Scientific, Inc. USA), digitized at 10 Hz and analyzed using Spike2 software (v 7.1, Cambridge Electronic Design, Cambridge, UK).

2.4. Immunohistochemistry

Ninety minutes after exposure to sham AIH or one of the three levels of AIH, rats underwent transcardiac perfusion with 4 °C solutions of heparinized saline (1000 U/mL, 100 mL) followed by 4% paraformaldehyde (PFA, 300 mL) in 0.2 M phosphate buffer (pH 7.4). Brains were removed, post-fixed at 4 °C for 4 h in PFA and transferred to 30% sucrose-PBS for ~2 days at 4 °C. Brains were sectioned in the coronal plane at 40 μm using a sliding microtome (Leica SM 2000R). Sections through the hypothalamus were collected into four serially adjacent sets and stored in polyvinyl-pyrrolidone cryoprotectant at −20 °C.

Detection of c-Fos: Immunostaining for c-Fos protein in neuronal nuclei was performed as described previously (Mitchell et al., 2018; Stocker et al., 2004; Stocker et al., 2006). Tissue sections through the PVN were removed from cryoprotectant and rinsed in 0.01 M PBS prior to incubation in 0.5% sodium borohydride for 30 min then in PBS containing 3% donkey serum and 0.3% Triton-X 100 for 2 h. Sections were then incubated with a polyclonal rabbit anti-rat c-Fos antibody (1:10,000; Millipore) at 4 °C for 72 h followed by incubation with biotinylated donkey anti-rabbit IgG (1:250; Vector Laboratories) for 2 h at room temperature. Sections were rinsed and incubated for 10 min with streptavidin-Alexa Fluor 594 (1:250; Invitrogen).

Neurochemical phenotyping: c-Fos stained sections underwent co-immunostaining for corticotropin-releasing hormone (CRH) or arginine vasopressin (AVP). Staining was compared between rats exposed to sham AIH and AIH to 8% O_2. The latter intensity of AIH was selected because it induced robust c-Fos expression in the PVN without eliciting obvious arousal behavior (see supplemental video file, S1). Hence c-Fos expression likely reflects neurons responsive to intermittent hypoxia rather than any behavioral consequences of hypoxic exposure.

To colocalize c-Fos amongst CRH or AVP containing neurons, c-Fos stained sections were incubated for 2 h in PBS containing 3% normal goat serum and 0.3% Triton-X 100 followed by incubation with a goat anti-rabbit IgG secondary antibody. Sections were then rinsed and incubated with polyclonal guinea pig anti-CRH or anti-AVP antibody (1:1000; Peninsula Laboratories). Sections were then rinsed and incubated for 2 h with a goat anti-guinea pig IgG secondary antibody (1:250; Invitrogen). Sections were again rinsed, then incubated for 10 min with streptavidin-Alexa Fluor 488 conjugate (1:250; Invitrogen).

Immunofluorescent images of PVN were captured using an inverted confocal microscope (Eclipse TE 2000E, Nikon) equipped with a 16-bit Andor Technology iXon camera. NIS-Elements AR software (v3.2) was used to mark and count neurons containing c-Fos, CRH and AVP immunofluorescence. Sub-divisions of the rat PVN were defined according to established criteria (Swanson and Kuypers, 1980).

2.5. Data analysis

For analysis of MAP and HR, values acquired each minute were averaged into 6 min bins, which is equivalent to the average during of each normoxia-hypoxia cycle. Values during sham and graded AIH were analyzed by two-way ANOVA followed by a layered Bonferroni *post hoc* test when indicated by a significant treatment x time interaction. The number of c-Fos stained nuclei as well as CRH or AVP stained soma were separately counted in representative sections from representative rostral, middle and caudal planes of the PVN. To quantify the proportion of CRH or AVP neurons activated by AIH, we related the size of each neuropeptide population (*i.e.*, total CRH + or AVP + counts) in the PVN to the size of the respective population that contained both CRH and c-Fos or AVP and c-Fos immunoreactivities (*i.e.*, double-labelled neurons). These ratios were expressed as the percent of the CRH or AVP cell population that was doubled labelled with c-Fos (see Fig. 3D).

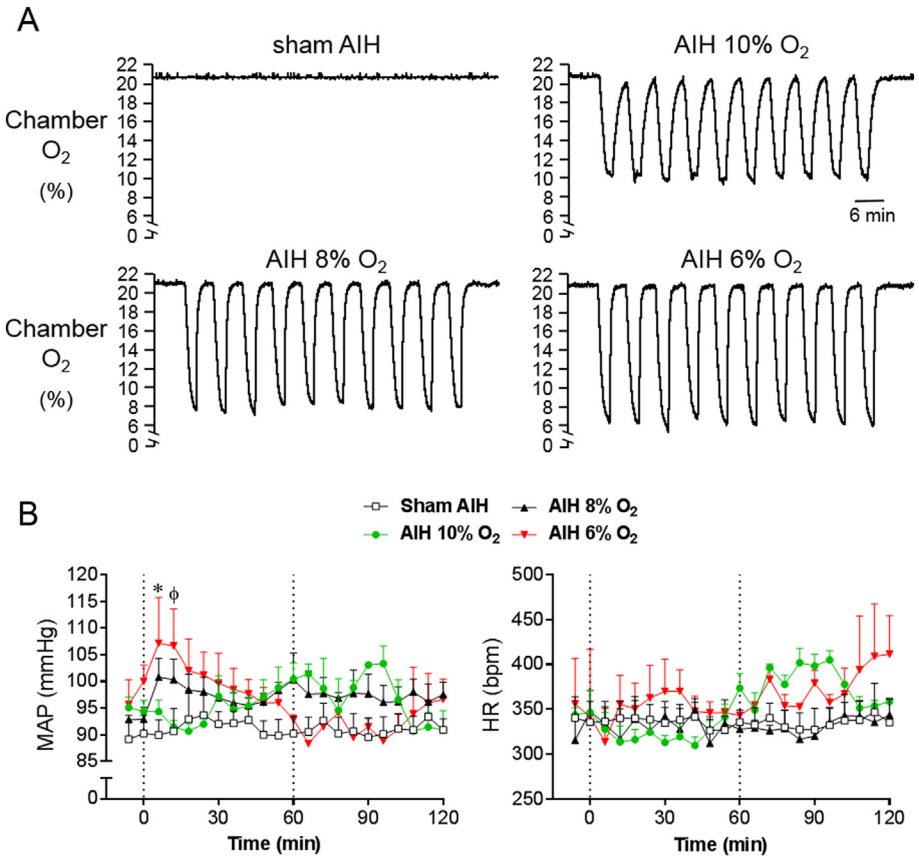

Fig. 1. Chamber O_2fluctuations and cardiovascular responses to graded AIH. (**A**) Representative traces of chamber O_2 concentration showing the pattern of O_2 changes during exposure to sham AIH (top, left) and graded intensities of AIH (bottom, right) over a period of 1 h. (**B**) Summary mean arterial pressure (MAP, left) and heart rate (HR, right) data at baseline and during exposure to sham and graded AIH (n = 4/group). MAP and HR were unaltered relative to baseline by sham AIH or AIH to 10% and 8% O_2. AIH to 6% O_2 was accompanied by modest and transient increase of MAP during cycles 1 and 2. * $P < 0.0017$, ϕ $P < 0.004$ *vs. corresponding time point in the sham AIH group. Dashed vertical lines indicate period of AIH exposure.*

Similarly, to quantify the proportions of AIH-activated PVN neurons that co-stained for CRH or AVP, we related the size of the AIH-activated neuron population (*i.e.*, total c-Fos+ counts) to the size of the neuron population that contained both c-Fos and CRH or c-Fos and AVP immunoreactivities (see Fig. 3E). At each rostro-caudal plane, counts were separated according to PVN subregions and compared between sham AIH and AIH to 10%, 8% and 6% O_2. Neurons in rostral, middle, and caudal planes of the PVN that were c-Fos-positive and double-labelled with CRF or AVP were separately counted. Total counts in each PVN subregion were estimated by summing region specific counts across the rostral, middle and caudal planes. Cell count data were analyzed by two-way ANOVA (GraphPad Prism 7.04 Software) followed by a layered Bonferroni post-hoc test when indicated by a significant treatment x time interaction. For all comparisons, a multiplicity error corrected critical value of $P < 0.05$ was considered statistically significant.

3. Results

3.1. Effects of AIH on blood pressure and heart rate

Conscious unrestrained rats were exposed to continuous normoxia (sham AIH) or to AIH protocols consisting of 10 normoxia-hypoxia cycles over a period of 1 h. Hypoxic episodes of AIH were to graded nadirs of 10%, 8% or 6% O_2 (Fig. 1A). Values of MAP and HR (Fig. 1B) remained stable during sham treatment and during AIH exposure to 10% and 8% O_2. AIH to 6% O_2 also failed to alter HR, but a significant increase of MAP relative to the sham group was detected [$F(3,156) = 11.58$, $P < 0.0001$], with pair-wise analysis indicating increased MAP limited to AIH cycles 1 ($P < 0.0017$) and 2 ($P < 0.004$). MAP and HR were stably maintained in the sham-AIH group during a 1 h post exposure period. By comparison, values in rats exposed to graded intensities of AIH were more variable, but not statistically different from those of the sham-AIH group.

3.2. Distribution of AIH responsive PVN neurons

Immunofluorescent staining of c-Fos was used to identify neurons in rostral, middle, and caudal planes of the PVN that were transcriptionally activated by AIH (Fig. 2A). Amongst rats exposed to sham AIH, c-Fos counts were sparse (total: 38 ± 12) and distributed nearly evenly through rostro-caudal planes of the PVN. A significant interaction between PVN subregions and graded intensities of AIH was detected [$F(9,80) = 18.89$, $P < 0.0001$], with c-Fos counts in the medial parvocellular (MP) region being significantly greater relative to sham treatment at each intensity of AIH (sham *vs.* 10%, $P < 0.0065$; sham *vs.* 8% and 6%, $P < 0.0001$). Analysis further revealed that c-Fos counts in the MP region progressively increased with increasing intensities of AIH (sham *vs.* 10%, $P < 0.0065$; 10% *vs.* 8%, $P < 0.005$; 8% *vs.* 6%, $P < 0.0001$). Relative to sham treatment, c-Fos counts also increased ($P < 0.05$) in the dorsal parvocellular (DP) and central magnocellular (CM) regions of the PVN, but only in response to AIH to 6% O_2. No level of AIH increased c-Fos counts in the caudally located lateral parvocellular (LP) region (Fig. 2B).

3.3. AIH activation of corticotropin releasing hormone (CRH) and arginine vasopressin (AVP) neurons

Given that exposure to graded intensities of AIH induced graded c-Fos counts only in the MP region of PVN, further analysis focused on determining the neurochemical phenotype(s) of activated MP neurons. Phenotyping focused on rats exposed to moderate AIH to 8% O_2 since these showed significant c-Fos expression in the MP region (Fig. 2B) without exhibiting obvious behavioral responses during hypoxic episodes (see video supplement, S1). Co-localization analysis focused on c-Fos amongst CRH and AVP expressing neurons since these are the

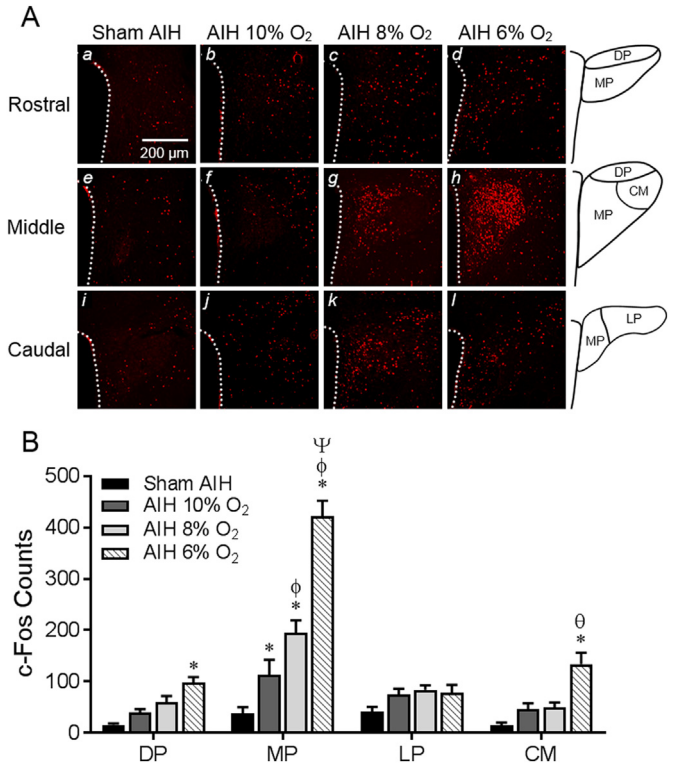

Fig. 2. Regional distribution of c-Fos in the PVN induced by exposure to AIH. (**A**) Representative images of rostral (*a-d*), middle (*e-h*) and caudal (*i-l*) planes through the PVN. Immunofluorescence of c-Fos staining is shown for rats exposed either to sham AIH (*a,e,i*) or AIH to 10% (*b,f,J*), 8% (*c,g,k*) and 6% (*d,h,l*) O_2. Line drawings (right column) depict PVN subregions. (**B**) Summary data (n = 6/group) of the number of c-Fos immunoreactive nuclei in PVN subregions summed across rostral, middle and caudal planes. AIH to graded nadirs of O_2 induced graded increases of c-Fos only in the MP subregion of PVN. c-Fos counts also increased in the DP and CM regions of PVN, but only in the group exposed to AIH to 6% O_2. *PVN subregions - DP, dorsal parvocellular; MP, medial parvocellular; LP, lateral parvocellular; CM, central magnocellular. Significance symbols indicate comparison within PVN subregion. * $P < 0.0065$ vs. sham AIH, ϕ $P < 0.005$ vs. 10% AIH, Ψ $P < 0.0001$ vs. 8% AIH, θ $P < 0.002$ vs. 10% and 8% AIH.*

dominant stress-regulatory cell types of the MP region of PVN (Herman et al., 1994; Lightman, 2008).

A significantly greater ($P < 0.0001$) number of MP neurons were immunoreactive for CRH than AVP (Fig. 3C), and count totals were unaffected by AIH to 8% O_2. Although AIH triggered c-Fos in a greater percentage of MP CRH ($P = 0.0013$) and AVP ($P = 0.0006$) neurons relative to sham treated controls, a similar percentage (~14%) of CRH and AVP stained neurons co-localized c-Fos in the AIH group (Fig. 3D). Further analysis revealed that the percentage of c-Fos stained neurons co-labelled with CRH or AVP was not different between sham treated and AIH exposed rats (Fig. 3E), indicating that c-Fos induced in response to AIH was not specific to these neuropeptide expressing neurons. Analysis further revealed that a significant fraction of AIH responsive (c-Fos positive) MP PVN neurons expressed CRH (~30%), but not AVP (~2%) (Fig. 3E).

3.4. Rostro-caudal distribution of MP CRH neurons activated by AIH

Because ~30% of c-Fos counts were localized to CRH neurons both in sham treated and AIH exposed rats (see Fig. 3D), AIH does not appear to selectively recruit CRH containing PVN neurons. However, AIH increased both the number (see Fig. 3C) and percentage (see Fig. 3D) of activated (c-Fos stained) CRH neurons without changing the size of the CRH neuron population. Data therefore indicate that AIH recruited ~12% more of the CRH neuron pool compared to sham treatment. With the latter in mind, we sought to determine if MP CRH neurons recruited by AIH were differentially distributed within the PVN. Figs. 4A shows that 83 ± 2% of c-Fos counts induced by AIH were located in the rostral half of the PVN, with significantly greater c-Fos counts located at the middle plane of the PVN compared to the rostral ($P = 0.0003$) or caudal planes ($P < 0.0001$). A similar pattern was observed for CRH stained neurons in which 80 ± 2% were located in the rostral half of the nucleus (Fig. 4B). In line with this pattern, 82 ± 2% of AIH-activated CRH stained neurons (double labelled) in the MP region were likewise located in the rostral one-half of the PVN, with a significantly greater number of double labelled neurons in the rostral ($P = 0.002$) and middle ($P = 0.02$) planes than the caudal plane of the PVN (Fig. 4C).

4. Discussion

Recent findings suggest that exposure to AIH activates PVN neurons (Blackburn et al., 2018). This interpretation is based on evidence in anesthetized rats that chemical inhibition of the PVN interferes both with bursts of sympathetic nerve activity (SNA) that accompany hypoxic episodes of AIH and with long-term facilitation of SNA (sLTF) that develops thereafter. But it is unknown whether these effects of PVN inhibition reflect interference with AIH stimulated discharge of PVN neurons or a reduction of ongoing PVN output signals that normally facilitate AIH-driven responses of neurons downstream. To address this knowledge gap, we used immunostaining of the immediate early gene product c-Fos to index transcriptional activation of PVN neurons when conscious rats were exposed to graded intensities of AIH.

In support of the view that AIH did indeed activate PVN neurons, graded AIH was found to induce graded increases in the number of c-Fos stained neuronal nuclei, but, interestingly, only in the MP subregion, which is densely populated with stress-related neurons in the rat (Coldren et al., 2017; Herman et al., 1995; Hwang et al., 2017; Wamsteeker and Bains, 2010). Of interest is that PVN neurons with monosynaptic connections to the spinal cord that regulate sympathetic outflow are dominantly located caudally in the PVN (Chen and Toney, 2003; Pyner and Coote, 2000; Sawchenko and Swanson, 1982; Stocker et al., 2006), and somewhat to our surprise AIH induced c-Fos expression in relative few neurons in the caudal LP region, suggesting that sympathetic responses to AIH are not likely to be relayed through these direct spinal projections.

Within the MP region, CRH stained neurons far outnumbered those stained for AVP. With this previously documented pattern (Lightman, 2008; Sawchenko et al., 1984) in mind, it is perhaps not surprising that a significant fraction of activated MP neurons (~30%) contained CRH, while a small minority (~2%) contained AVP. Together with existing literature evidence (Ma et al., 2008; Przygodda et al., 2017; Xing and Pilowsky, 2010), these findings suggest that MP CRH neurons could represent a synaptic nodal point within an AIH responsive network. Insight into the circuitry activated by AIH has been provided in a recent report (Kim et al., 2018), which revealed a critical role for the circulating hormone angiotensin II (AngII) in triggering AIH-induced sLTF. According to that study, AIH increases blood borne AngII, which then acts both at carotid body chemoreceptors to sensitize their activation by hypoxemia (Fung, 2015; Marcus et al., 2010; Schultz, 2011), and at the blood-brain-barrier deficient forebrain subfornical organ (SFO) (Anderson et al., 2001; Ferguson, 2009). This model of sLTF is consistent with involvement of PVN neurons because they receive inputs both from arterial chemoreceptor responsive neurons in the nucleus tractus solitarius (NTS) (Coldren et al., 2017; King et al., 2012; King et al., 2015; Reddy et al., 2005; Reddy et al., 2007) and from AngII responsive neurons in the SFO (Bains et al., 1992; King et al., 2012).

The extent to which CRH neurons expressed c-Fos specifically in response to these AngII-facilitated AIH-driven inputs is presently unknown. If they did, an important question is whether CRH neuronal

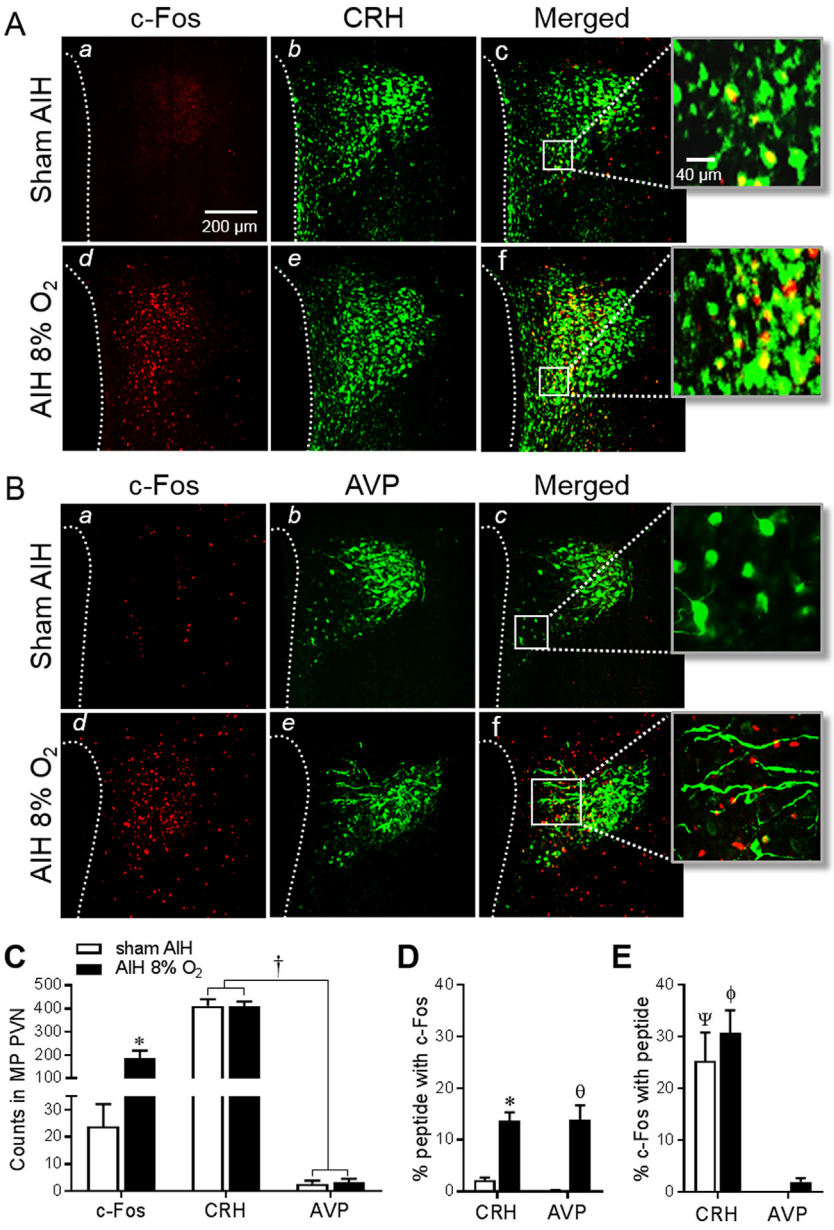

Fig. 3. Co-localization of AIH-induced c-Fos with stress-regulatory neuropeptides. Images of c-Fos stained sections (*a,d, red*) in the MP region of PVN following exposure to sham AIH and AIH to 8% O_2. Sections were co-stained (*b,e, green*) for CRH (**A**) or AVP (**B**) and merged images (*c,f*) show c-Fos co-localization with CRH or AVP. Higher magnification (40×) images (far right) show double labelled neurons in yellow. (**C**) Summary data (n = 6/group) of c-Fos, CRH and AVP immunoreactive counts in the MP region of PVN. (**D**) AIH induced c-Fos in a similar fraction of CRH and AVP neurons. (**E**) The fraction of c-Fos positive MP PVN neurons that expressed CRH was similar in sham and AIH exposed rats, and these were each significantly greater than the fraction immunoreactive for AVP. * $P < 0.005$, θ $P = 0.0006$ *vs. sham AIH,* † $P < 0.0001$, Ψ $P = 0.0035$, ϕ $P = 0.0005$ *vs. corresponding AVP value.* (For interpretation of the references to colour in this figure legend, the reader is referred to the web version of this article.)

activation (with or without exposure to AIH) would be sufficient to recapitulate sLTF-like ramping of SNA. Support for this possibility stems from our previous study in which a progressive increase of splanchnic SNA was elicited by hyperglycemia (Bardgett et al., 2014b). In that study, the slope of the SNA ramp was similar to that of post-AIH sLTF, and the ramp was largely prevented by prior blockade of CRH receptors in the brainstem RVLM. Given that the RVLM is a known downstream target of CRH neurons in the PVN (Bardgett et al., 2014b; Van Kempen et al., 2015), activation of a PVN-RVLM CRHergic pathway appears capable of triggering a ramp-like increase of SNA that resembles the sLTF response.

It should be stressed that most PVN-RVLM neurons express vGlut2 (Stocker et al., 2006), a marker of glutamatergic neurons, which suggests that RVLM-projecting CRHergic neurons are likely also glutamatergic. Consequently, ramp increases of SNA caused by activating this pathway, possibly by AIH, could reflect an interaction in the RVLM between CRH receptor signaling and glutamatergic transmission (Marcus et al., 2010). Such interactions have been documented for hippocampal CA1 pyramidal neuron responses to Schaffer collateral inputs from the CA3 region (Kratzer et al., 2013).

As noted, the present study found that ~30% of AIH-activated MP neurons contained CRH and exceeding few contained AVP. The neurochemical identity of the remaining ~70% of AIH responsive PVN neurons is unknown. Within the MP region, neurons express a host of neuropeptides including oxytocin (Kita et al., 2006; Lee et al., 2013), dynorphin (Lee et al., 2013), somatostatin (Swanson and Sawchenko, 1983), neurotensin (Goedert et al., 1985) and substance P (Argiolas and Melis, 2013; Nunn et al., 2011), along with a population of dopaminergic neurons (Swanson and Sawchenko, 1983; Swanson et al., 1981). Which of these might be responsive to AIH is unknown, and what role they might play in transmitting sLTF signals remains to be investigated.

Most AIH-activated PVN neurons were located in the rostral half of the nucleus. This distribution has potentially important implications because neurons in the rostral and middle portions of PVN, in addition to projecting to the brainstem to regulate SNA (Stocker et al., 2004; Stocker et al., 2006; Swanson and Kuypers, 1980), comprise neuroendocrine cells of the HPA axis and are thus critical for responding to a host of stressors (Lightman, 2008; Wamsteeker and Bains, 2010). This is important because stress responsive PVN neurons are known to also project to limbic regions (Li and Sawchenko, 1998; Rodaros et al.,

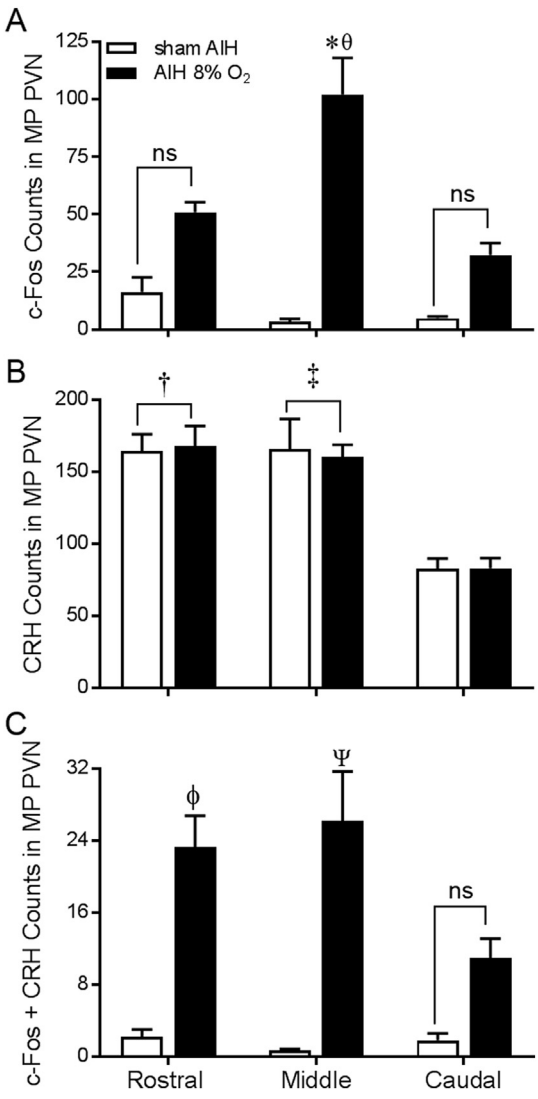

Fig. 4. Distribution of AIH responsive CRH neurons. Cell counts of neurons individually stained for c-Fos (**A**) and CRH (**B**) in rostral, middle and caudal planes of the MP PVN of rats exposed to sham AIH (n = 6, open bars) and AIH to 8% O_2 (n = 6, filled bars). (**C**) Rostro-caudal distribution of double-labelled MP PVN neurons containing c-Fos and CRH immunoreactivity. * *P = 0.0003 vs rostral value in AIH group; θ P < 0.0001 vs caudal value in AIH group and middle value in sham group; † P < 0.002, ‡ P < 0.003 vs corresponding caudal values; ϕ P = 0.002 vs rostral value in sham group; Ψ P = 0.02 vs. within group caudal value.*

2007; Sofroniew, 1980), which suggest possible roles in modulating mood (Bao and Swaab, 2010; Mitchell et al., 2018; Scott and Dinan, 1998; Veenema and Neumann, 2008) as well as memory acquisition and retention (Bergstrom, 2016). Hence AIH exposure may constitute a stressor that modulates a host of functionally significant endpoints, possibly by triggering widespread neuroplasticity through mechanisms in common with those that result in post-AIH sLTF.

To our knowledge, this study is the first to have recorded MAP and HR responses to graded intensities of AIH in conscious unrestrained rats using radio telemetry. We found that graded levels AIH did not affect HR, and caused a modest and transient rise of MAP only in animals exposed to the most hypoxic level of AIH examined (*i.e.*, nadirs of 6% O_2). More pronounced cardiovascular effects of AIH have been reported in anesthetized rats (Blackburn et al.; Kim et al., 2018), and these are likely explained by one or more of the following: (1) Anesthesia-induced blunting of arterial chemoreflex sympathoexcitation, which could have permitted more pronounced depressor effects of hypoxic vasodilation (Marcus et al., 2009). (2) Inability of anesthetized animals to hyperventilate during hypoxic episodes due to chemical paralysis and artificial ventilation. (3) Interruption of pulmonary and cardiac viscero-sensory inputs as well as cardio-motor inhibitory outflow due to bilateral cervical vagotomy.

Of interest is that development of sLTF during the post-AIH period in anesthetized rats is not accompanied by significant effects on HR and is inconsistently accompanied by an increase of MAP (Blackburn et al., 2018; Kim et al., 2018; Xing and Pilowsky, 2010; Xing et al., 2014). Here, we recorded HR and MAP in conscious rats during a 1 h post-AIH period and found that neither HR nor MAP was significantly altered relative to baseline. Whether this indicates that any increase of SNA that may have occurred during the post-AIH period (*i.e.*, sLTF) was dominated by non-vasomotor activity is presently unknown. It is also possible that autonomic reflexes as well as peripheral vascular and cardio-regulatory mechanisms active during the post-AIH period could have offset any tachycardic and pressor effects of sLTF that might otherwise have been observed. Finally, we cannot presently rule out the possibility that failure of HR and MAP to change during the post-AIH period in conscious rats might reflect failure of AIH to trigger sLTF.

Favoring the likelihood that AIH in conscious animals can trigger sLTF is evidence that intermittent optogenetic activation of the caudal NTS, where arterial chemoreceptor afferent inputs terminate, triggers an sLTF-like response without causing repetitive reductions of MAP (renal perfusion pressure) (Yamamoto et al., 2015). This is significant because repetitive reductions of MAP during AIH presumably aid activation of the peripheral renin-angiotensin-system, which has recently been reported in anesthetized rats to be essential for triggering post-AIH sLTF (Kim et al., 2018). Studies in conscious humans also indicate that repetitive voluntary apneas that are not accompanied by reductions of MAP can also trigger a long-lasting elevation of SNA, resembling the sLTF response (Cutler et al., 2004). The above findings suggest that elevated plasma AngII during AIH may not depend on renin released in response to reduced MAP. Definitive evidence that AIH induces sLTF in conscious animals will require stable recording of SNA during and after AIH, which poses a daunting technical challenge given available nerve recording technology.

In summary, results of the present study indicate that exposure of conscious rats to graded intensities of AIH elicits only muted cardiovascular responses, but triggers graded c-Fos activation amongst PVN neurons in the rostral half of the medial parvocellular region of the nucleus. The neurochemical identity of most AIH responsive PVN neurons remains to be determined, but findings reveal a significant population of responsive neurons contain the neuropeptide CRH. These neurons likely contribute to AIH-induced activation of endocrine and autonomic components of the stress response. Additional studies are needed to precisely define the role these CRH neurons play in AIH-induced sLTF neuroplasticity.

Acknowledgements

The authors thank Ms. Mary Ann Andrade for excellent technical assistance and Dr. Allison Brackley for video editing. We also thank Drs. Steven Mifflin and J. Thomas Cunningham for helpful discussions during the course of these studies.

Grants

This work was supported by NIH (NHLBI) Grant HL088052 and American Heart Association Grant 25,710,176 (GMT). NCM received stipend support from NIH (NHLBI) T32 HL07446.

Disclosures

The authors have no conflicts of interest to declare.

References

Anderson, J.W., Smith, P.M., Ferguson, A.V., 2001. Subfornical organ neurons projecting to paraventricular nucleus: whole-cell properties. Brain Res. 921, 78–85.

Arango-Lievano, M., Lambert, W.M., Bath, K.G., Garabedian, M.J., Chao, M.V., Jeanneteau, F., 2015. Neurotrophic-priming of glucocorticoid receptor signaling is essential for neuronal plasticity to stress and antidepressant treatment. Proc. Natl. Acad. Sci. U. S. A. 112, 15737–15742.

Argiolas, A., Melis, M.R., 2013. Neuropeptides and central control of sexual behaviour from the past to the present: a review. Prog. Neurobiol. 108, 80–107.

Bains, J.S., Potyok, A., Ferguson, A.V., 1992. Angiotensin II actions in paraventricular nucleus: functional evidence for neurotransmitter role in efferents originating in subfornical organ. Brain Res. 599, 223–229.

Bao, A.M., Swaab, D.F., 2010. Corticotropin-releasing hormone and arginine vasopressin in depression focus on the human postmortem hypothalamus. Vitam. Horm. 82, 339–365.

Bardgett, M.E., Holbein, W.W., Herrera-Rosales, M., Toney, G.M., 2014a. Ang II-salt hypertension depends on neuronal activity in the hypothalamic paraventricular nucleus but not on local actions of tumor necrosis factor-alpha. Hypertension 63, 527–534.

Bardgett, M.E., Sharpe, A.L., Toney, G.M., 2014b. Activation of corticotropin-releasing factor receptors in the rostral ventrolateral medulla is required for glucose-induced sympathoexcitation. Am. J. Physiol. Endocrinol. Metab. 307, E944–E953.

Bergstrom, H.C., 2016. The neurocircuitry of remote cued fear memory. Neurosci. Biobehav. Rev. 71, 409–417.

Blackburn, M.B., Andrade, M.A., Toney, G.M., 2018. Hypothalamic PVN contributes to acute intermittent hypoxia-induced sympathetic but not phrenic long-term facilitation. J. Appl. Physiol. (1985) 124, 1233–1243.

Chen, Q.H., Toney, G.M., 2003. Identification and characterization of two functionally distinct groups of spinal cord-projecting paraventricular nucleus neurons with sympathetic-related activity. Neuroscience 118, 797–807.

Coldren, K.M., Li, D.P., Kline, D.D., Hasser, E.M., Heesch, C.M., 2017. Acute hypoxia activates neuroendocrine, but not presympathetic, neurons in the paraventricular nucleus of the hypothalamus: differential role of nitric oxide. Am. J. Physiol. Regul. Integr. Comp. Physiol. 312, R982–R995.

Cutler, M.J., Swift, N.M., Keller, D.M., Wasmund, W.L., Smith, M.L., 2004. Hypoxia-mediated prolonged elevation of sympathetic nerve activity after periods of intermittent hypoxic apnea. J. Appl. Physiol. (1985) 96, 754–761.

Dick, T.E., Hsieh, Y.H., Wang, N., Prabhakar, N., 2007. Acute intermittent hypoxia increases both phrenic and sympathetic nerve activities in the rat. Exp. Physiol. 92, 87–97.

Ferguson, A.V., 2009. Angiotensinergic regulation of autonomic and neuroendocrine outputs: critical roles for the subfornical organ and paraventricular nucleus. Neuroendocrinology 89, 370–376.

Fung, M.L., 2015. Expressions of angiotensin and cytokine receptors in the paracrine signaling of the carotid body in hypoxia and sleep apnea. Respir. Physiol. Neurobiol. 209, 6–12.

Goedert, M., Lightman, S.L., Mantyh, P.W., Hunt, S.P., Emson, P.C., 1985. Neurotensin-like immunoreactivity and neurotensin receptors in the rat hypothalamus and in the neurointermediate lobe of the pituitary gland. Brain Res. 358, 59–69.

Herman, J.P., Cullinan, W.E., Watson, S.J., 1994. Involvement of the bed nucleus of the stria terminalis in tonic regulation of paraventricular hypothalamic CRH and AVP mRNA expression. J. Neuroendocrinol. 6, 433–442.

Herman, J.P., Adams, D., Prewitt, C., 1995. Regulatory changes in neuroendocrine stress-integrative circuitry produced by a variable stress paradigm. Neuroendocrinology 61, 180–190.

Hwang, G.S., Chen, C.C., Chou, J.C., Chang, L.L., Kan, S.F., Lai, W.H., Lieu, F.K., Hu, S., Wang, P.S., Wang, S.W., 2017. Stimulatory effect of Intermittent Hypoxia on the production of Corticosterone by Zona Fasciculata-Reticularis Cells in Rats. Sci. Rep. 7, 9035.

Kim, S.J., Fong, A.Y., Pilowsky, P.M., Abbott, S.B.G., 2018. Sympathoexcitation following intermittent hypoxia in rat is mediated by circulating angiotensin II acting at the carotid body and subfornical organ. J. Physiol. 596 (15), 3217–3232.

King, T.L., Heesch, C.M., Clark, C.G., Kline, D.D., Hasser, E.M., 2012. Hypoxia activates nucleus tractus solitarii neurons projecting to the paraventricular nucleus of the hypothalamus. Am. J. Physiol. Regul. Integr. Comp. Physiol. 302, R1219–R1232.

King, T.L., Ruyle, B.C., Kline, D.D., Heesch, C.M., Hasser, E.M., 2015. Catecholaminergic neurons projecting to the paraventricular nucleus of the hypothalamus are essential for cardiorespiratory adjustments to hypoxia. Am. J. Physiol. Regul. Integr. Comp. Physiol. 309, R721–R731.

Kita, I., Yoshida, Y., Nishino, S., 2006. An activation of parvocellular oxytocinergic neurons in the paraventricular nucleus in oxytocin-induced yawning and penile erection. Neurosci. Res. 54, 269–275.

Kratzer, S., Mattusch, C., Metzger, M.W., Dedic, N., Noll-Hussong, M., Kafitz, K.W., Eder, M., Deussing, J.M., Holsboer, F., Kochs, E., Rammes, G., 2013. Activation of CRH receptor type 1 expressed on glutamatergic neurons increases excitability of CA1 pyramidal neurons by the modulation of voltage-gated ion channels. Front. Cell. Neurosci. 7, 91.

Lee, S.K., Ryu, P.D., Lee, S.Y., 2013. Differential distributions of neuropeptides in hypothalamic paraventricular nucleus neurons projecting to the rostral ventrolateral medulla in the rat. Neurosci. Lett. 556, 160–165.

Li, H.Y., Sawchenko, P.E., 1998. Hypothalamic effector neurons and extended circuitries activated in "neurogenic" stress: a comparison of footshock effects exerted acutely, chronically, and in animals with controlled glucocorticoid levels. J. Comp. Neurol. 393, 244–266.

Lightman, S.L., 2008. The neuroendocrinology of stress: a never ending story. J. Neuroendocrinol. 20, 880–884.

Ma, S., Mifflin, S.W., Cunningham, J.T., Morilak, D.A., 2008. Chronic intermittent hypoxia sensitizes acute hypothalamic-pituitary-adrenal stress reactivity and Fos induction in the rat locus coeruleus in response to subsequent immobilization stress. Neuroscience 154, 1639–1647.

Marcus, N.J., Olson Jr., E.B., Bird, C.E., Philippi, N.R., Morgan, B.J., 2009. Time-dependent adaptation in the hemodynamic response to hypoxia. Respir. Physiol. Neurobiol. 165, 90–96.

Marcus, N.J., Li, Y.L., Bird, C.E., Schultz, H.D., Morgan, B.J., 2010. Chronic intermittent hypoxia augments chemoreflex control of sympathetic activity: role of the angiotensin II type 1 receptor. Respir. Physiol. Neurobiol. 171, 36–45.

Miselis, R.R., 1981. The efferent projections of the subfornical organ of the rat: a circumventricular organ within a neural network subserving water balance. Brain Res. 230, 1–23.

Mitchell, N.C., Gilman, T.L., Daws, L.C., Toney, G.M., 2018. High salt intake enhances swim stress-induced PVN vasopressin cell activation and active stress coping. Psychoneuroendocrinology 93, 29–38.

Nunn, N., Womack, M., Dart, C., Barrett-Jolley, R., 2011. Function and pharmacology of spinally-projecting sympathetic pre-autonomic neurones in the paraventricular nucleus of the hypothalamus. Curr. Neuropharmacol. 9, 262–277.

Peters, A., Reisch, C., Langemann, D., 2018. LTP or LTD? Modeling the Influence of stress on Synaptic Plasticity. eNeuro 5.

Przygodda, F., Manfredi, L.H., Machado, J., Goncalves, D.A.P., Zanon, N.M., Bonagamba, L.G.H., Machado, B.H., Kettelhut, I.C., Navegantes, L.C.C., 2017. Acute intermittent hypoxia in rats activates muscle proteolytic pathways through a gluccorticoid-dependent mechanism. J Appl Physiol (1985) 122, 1114–1124.

Pyner, S., Coote, J.H., 2000. Identification of branching paraventricular neurons of the hypothalamus that project to the rostroventrolateral medulla and spinal cord. Neuroscience 100, 549–556.

Reddy, M.K., Patel, K.P., Schultz, H.D., 2005. Differential role of the paraventricular nucleus of the hypothalamus in modulating the sympathoexcitatory component of peripheral and central chemoreflexes. Am. J. Physiol. Regul. Integr. Comp. Physiol. 289, R789–R797.

Reddy, M.K., Schultz, H.D., Zheng, H., Patel, K.P., 2007. Altered nitric oxide mechanism within the paraventricular nucleus contributes to the augmented carotid body chemoreflex in heart failure. Am. J. Physiol. Heart Circ. Physiol. 292, H149–H157.

Rodaros, D., Caruana, D.A., Amir, S., Stewart, J., 2007. Corticotropin-releasing factor projections from limbic forebrain and paraventricular nucleus of the hypothalamus to the region of the ventral tegmental area. Neuroscience 150, 8–13.

Sawchenko, P.E., Swanson, L.W., 1982. Immunohistochemical identification of neurons in the paraventricular nucleus of the hypothalamus that project to the medulla or to the spinal cord in the rat. J. Comp. Neurol. 205, 260–272.

Sawchenko, P.E., Swanson, L.W., Vale, W.W., 1984. Co-expression of corticotropin-releasing factor and vasopressin immunoreactivity in parvocellular neurosecretory neurons of the adrenalectomized rat. Proc. Natl. Acad. Sci. U. S. A. 81, 1883–1887.

Schierloh, A., Deussing, J., Wurst, W., Zieglgansberger, W., Rammes, G., 2007. Corticotropin-releasing factor (CRF) receptor type 1-dependent modulation of synaptic plasticity. Neurosci. Lett. 416, 82–86.

Schultz, H.D., 2011. Angiotensin and carotid body chemoreception in heart failure. Curr. Opin. Pharmacol. 11, 144–149.

Scott, L.V., Dinan, T.G., 1998. Vasopressin and the regulation of hypothalamic-pituitary-adrenal axis function: implications for the pathophysiology of depression. Life Sci. 62, 1985–1998.

Sharpe, A.L., Andrade, M.A., Herrera-Rosales, M., Britton, S.L., Koch, L.G., Toney, G.M., 2013a. Rats selectively bred for differences in aerobic capacity have similar hypertensive responses to chronic intermittent hypoxia. Am. J. Physiol. Heart Circ. Physiol. 305, H403–H409.

Sharpe, A.L., Calderon, A.S., Andrade, M.A., Cunningham, J.T., Mifflin, S.W., Toney, G.M., 2013b. Chronic intermittent hypoxia increases sympathetic control of blood pressure: role of neuronal activity in the hypothalamic paraventricular nucleus. Am. J. Physiol. Heart Circ. Physiol. 305, H1772–H1780.

Sofroniew, M.V., 1980. Projections from vasopressin, oxytocin, and neurophysin neurons to neural targets in the rat and human. J. Histochem. Cytochem. 28, 475–478.

Stocker, S.D., Cunningham, J.T., Toney, G.M., 2004. Water deprivation increases Fos immunoreactivity in PVN autonomic neurons with projections to the spinal cord and rostral ventrolateral medulla. Am. J. Physiol. Regul. Integr. Comp. Physiol. 287, R1172–R1183.

Stocker, S.D., Simmons, J.R., Stornetta, R.L., Toney, G.M., Guyenet, P.G., 2006. Water deprivation activates a glutamatergic projection from the hypothalamic paraventricular nucleus to the rostral ventrolateral medulla. J. Comp. Neurol. 494, 673–685.

Swanson, L.W., Kuypers, H.G., 1980. The paraventricular nucleus of the hypothalamus: cytoarchitectonic subdivisions and organization of projections to the pituitary, dorsal vagal complex, and spinal cord as demonstrated by retrograde fluorescence double-labeling methods. J. Comp. Neurol. 194, 555–570.

Swanson, L.W., Sawchenko, P.E., 1983. Hypothalamic integration: organization of the paraventricular and supraoptic nuclei. Annu. Rev. Neurosci. 6, 269–324.

Swanson, L.W., Sawchenko, P.E., Berod, A., Hartman, B.K., Helle, K.B., Vanorden, D.E., 1981. An immunohistochemical study of the organization of catecholaminergic cells and terminal fields in the paraventricular and supraoptic nuclei of the hypothalamus. J. Comp. Neurol. 196, 271–285.

Van Kempen, T.A., Dodos, M., Woods, C., Marques-Lopes, J., Justice, N.J., Iadecola, C., Pickel, V.M., Glass, M.J., Milner, T.A., 2015. Sex differences in NMDA GluN1 plasticity in rostral ventrolateral medulla neurons containing corticotropin-releasing factor type 1 receptor following slow-pressor angiotensin II hypertension.

Neuroscience 307, 83–97.
Veenema, A.H., Neumann, I.D., 2008. Central vasopressin and oxytocin release: regulation of complex social behaviours. Prog. Brain Res. 170, 261–276.
Wamsteeker, J.I., Bains, J.S., 2010. A synaptocentric view of the neuroendocrine response to stress. Eur. J. Neurosci. 32, 2011–2021.
Wang, T.Y., Chen, X.Q., Du, J.Z., Xu, N.Y., Wei, C.B., Vale, W.W., 2004. Corticotropin-releasing factor receptor type 1 and 2 mRNA expression in the rat anterior pituitary is modulated by intermittent hypoxia, cold and restraint. Neuroscience 128, 111–119.
Xing, T., Pilowsky, P.M., 2010. Acute intermittent hypoxia in rat in vivo elicits a robust increase in tonic sympathetic nerve activity that is independent of respiratory drive. J. Physiol. 588, 3075–3088.
Xing, T., Pilowsky, P.M., Fong, A.Y., 2014. Mechanism of sympathetic activation and blood pressure elevation in humans and animals following acute intermittent hypoxia. Prog. Brain Res. 209, 131–146.
Yamamoto, K., Lalley, P., Mifflin, S., 2015. Acute intermittent optogenetic stimulation of nucleus tractus solitarius neurons induces sympathetic long-term facilitation. Am. J. Physiol. Regul. Integr. Comp. Physiol. 308, R266–R275.
Zoccal, D.B., Bonagamba, L.G., Antunes-Rodrigues, J., Machado, B.H., 2007. Plasma corticosterone levels is elevated in rats submitted to chronic intermittent hypoxia. Auton. Neurosci. 134, 115–117.